Vibrational properties of amorphous germanium under pressure and its thermal expansion and Grüneisen parameters

Murat Durandurdu *

Department of Physics, University of Texas at El Paso, El Paso, TX 79968, USA
Fizik Bölümü, Ahi Evran Üniversitesi, Kırşehir 40100, Turkey

ARTICLE INFO

ABSTRACT

We study the vibrational properties of amorphous germanium at high pressures using a constant pressure *ab initio* technique. With the application of pressure, the low-frequency modes gradually soften with a decrease in their acoustic-like nature while the high-frequency modes shift to larger frequencies. The acoustic-like vibrations are found to have negative Grüneisen parameters whereas the optic-like ones have positive values of about +1. A negative thermal expansion is produced below 200 K. Furthermore, we find that pressure reduces the number of localized states. Accompanied by the phase transition into a metallic high-density amorphous state, the nature of the low-frequency vibrations is changed from acoustic-like to optic-like and from bond bending to bond stretching.

© 2010 Elsevier B.V. All rights reserved.

1. Introduction

Amorphous semiconductors are of technological importance for electronic and optoelectronic device applications. In the past decades, numerous experimental and theoretical investigations [1–14] have been performed to better understand electronic and vibrational properties of amorphous materials and much progress has been made. However, local structural changes due to external perturbations and their relations to other physical properties of amorphous networks are still not well-understood. In this study, we use a first-principles pseudopotential technique to investigate the influence of pressure on the vibrational spectrum of amorphous germanium (*a*-Ge). The characterization of the phonon spectrum of *a*-Ge under pressure is important for understanding not only the structure of *a*-Ge itself but all topologically similar amorphous materials. Furthermore, such an investigation might be helpful in understanding pressure-induced amorphous-to-amorphous phase transition and an anomalous negative thermal expansion observed in some tetrahedrally bonded amorphous materials [9].

The vibrational spectrum of amorphous semiconductors such as germanium and silicon is sensitive to sample preparation techniques, degree of structural disorder, deposition conditions and hydrogen concentration [1–3]. The intensity of bands and their lines width correlate with the bond angle distribution of samples

[3,4]. Moreover, the number of localized states is found to be associated with the density of amorphous systems [5–8].

Polyamorphism [15] refers to distinct amorphous states with different densities and bonding environments and is of interest both as a scientific phenomenon and because of its implications in materials processing. For amorphous materials, it can be typically obtained by increasing external pressure. The density driven amorphous-to-amorphous phase transformation has been studied extensively [16–37] and occurs in a variety of systems. The existence of multiple amorphous phases has revived the idea of an underlying liquid–liquid phase transition, indicating the existence of a low-density liquid and its glass transition to the amorphous solids [20].

Both theoretical and experimental studies [21–24] have provided enough solid evidence for the existence of such a phase transformation from a low-density semiconducting phase to a high density metallic amorphous phase in *a*-Ge with the application of pressure. In these studies, however, the influence of pressure on the vibrational properties has not been reported. In this paper, we study the phonon spectrum of *a*-Ge under pressure using *ab initio* constant pressure simulations and lattice dynamical calculations. We find that pressure softens the low-energy modes and decreases their acoustic-like nature. The low-frequency states are calculated to have negative Grüneisen parameters. Consequently, a negative thermal expansion is observed in *a*-Ge below 200 K. On the other hand, the high-frequency vibrations increase linearly with the application of pressure and have positive Grüneisen parameters. We also find that the localized states at zero-pressure become extended with increasing pressure. Furthermore, we observe that the nature of the low-frequency modes is changed from

* Address: Department of Physics, University of Texas at El Paso, El Paso, TX 79968, USA.
  E-mail address: mdurandurdu@utep.edu

acoustic-like to optic-like and from bond bending to bond stretching when the low-density semiconducting *a*-Ge transforms into a metallic high-density amorphous state.

2. Methodology

The model used here is generated using an improved version of the Wooten–Winer–Weaire algorithm [38]. At zero-pressure, the model is equilibrated and relaxed with the local orbital first principles quantum molecular dynamics method of Sankey and Niklewski [39]. The energy difference between the diamond and the amorphous model is found to be 150 meV/atom in agreement with 120 meV/atom from a heat crystallization measurement [40,41]. This Hamiltonian was successfully applied to study the pressure-induced phase transition crystalline Ge [42]. Pressure is applied by the Parrinello–Rahman method [43] and it is increased by an increment of 2 GPa up to 12 GPa, after which an increment of 0.25 GPa is carried out in order to accurately estimate the transition pressure. Under constant pressure, the system is fully relaxed according to the criterion that the maximum force is smaller than 0.01 eV/Å. We use Γ-point sampling for the supercell's Brillouin zone integration, which is reasonable for a 216-atom model. A fictitious cell mass of 16×10^3 amu was found to be suitable for these simulations.

Once the equilibrium configurations under pressure are obtained, we compute the dynamical matrix, displacing every atom in the cell in three orthogonal directions (0.03 Å) and computing the resulting spring constants as second derivatives of the total energy of the system. Diagonalizing the dynamical matrix we receive its eigenvectors and corresponding squared normal-mode frequencies ω^2, which allow us to perform a detailed mode analysis of the high pressure configurations.

3. Results

3.1. Structural properties

We first briefly summarize the structural properties of *a*-Ge as a function of pressure in Table 1. The detail of the simulations can be found in Ref. [21]. The compression noticeably narrows tetrahedral angles and shortens bond lengths but the structure remains four-fold coordinated up to 12.75 GPa at which point the *a*-Ge model undergoes a first order phase transformation from a semiconducting low-density amorphous phase to a metallic high-density amorphous phase. The metallic high-pressure phase consists of differently bounded domains and resemblances to liquid Ge [21].

3.2. Vibrational density of states

The computed vibrational density of states (VDOS) of the model at several pressures is shown in Fig.1. At zero-pressure, the model shows no vibrational states below 60 cm^{-1} because of the finite size of the simulation cell: small **k** modes are missing from the simulation, which are strictly zone centered. As the model is com-
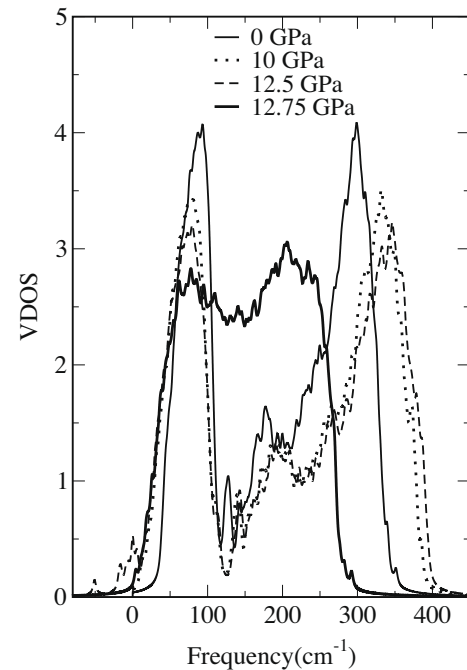

Fig. 1. The behavior of the VDOS under pressure.

pressed gradually, the low-frequency modes shift continuously to smaller-energies. Near the transition pressure, instability occurs in the system, which leads to imaginary frequencies. We multiplied the imaginary frequencies by *i* so that they show up on the negative real frequency axis. The modes in the high-frequency range, on the other hand, move toward larger energies with the application of pressure. At the transition pressure of 12.75 GPa, the modes decrease to values that are lower than those of the initial amorphous configuration.

The imaginary frequencies near the transition pressure can be viewed as an artifact of the simulation because of the overpressurizing system. Namely, in order to observe a structural phase transformation in simulations, systems must be overpressurized because of the use of finite size of simulation boxes with periodic boundary conditions (the absence of surfaces in simulated structure). In the simulation, the imaginary frequencies however can be interpreted as a structural instability of networks [44] and useful for an indication of a phase transition in this type of simulation [5].

The frequencies near 300 cm^{-1}, on the other hand, gradually shift to higher frequencies with increasing pressure as a consequence of the bond shortening. This observation is in good agreement with the recent Raman studies [22,45]. As the system undergoes the amorphous-to-amorphous phase transition, the high frequency band shifts to the lover frequencies with a dramatic decrease in its intensity, which is again consisting with the Raman study in which the loss of Raman signals was observed when the sample transforms into a HDA phase.

3.3. Grüneisen parameters

Softening of the low-frequencies modes with increasing pressure (decreasing volume) indicates that the low-frequency vibrations of *a*-Ge have negative Grüneisen parameters γ_n that describe the scaling of phonon frequencies ω_n with volume *V*, which might depend on pressure *P*:

Table 1
Structural properties of *a*-Ge on compression: average bond length (ABL), average bond angle (ABA), width of bond angle distribution (WBAD), and average coordination number (ACN).

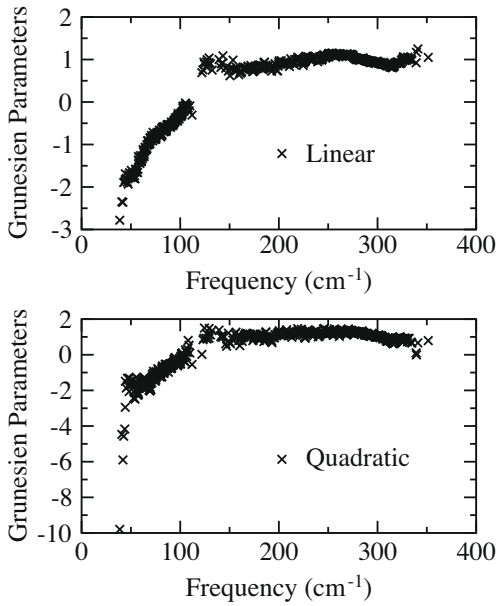| Pressure (GPa)	0	8	10	12.5	12.75
ABL (Å)	2.421	2.357	2.345	2.332	2.6338
ABA (°)	109.16	108.98	108.90	108.71	98.81
WBAD	10.18	11.09	11.46	12.28	32.37
ACN	4.0	4.0	4.0	4.0	8.03

Fig. 2. Calculated Grüneisen parameters.

$$\gamma_n = -\left[\frac{d\ln\omega_n}{d\ln V}\right]_{V(P)} = \frac{B}{\omega_n}\left[\frac{d\omega_n}{dP}\right]_T,$$

where B is the isothermal bulk modulus and calculated to be 73 GPa for the a-Ge model [21].

We determine the frequency–pressure relation using both linear and quadratic fits in the pressure-range 0–8 GPa in which no imaginary frequency exists, and then we calculate γ_n. Due to the fitting, some errors are expected in our calculations. Fig. 2 shows the computed Grüneisen parameters. Accordingly, the acoustic-like phonons below 120 cm^{-1} have negative γ_n while the optic-like ones have positive γ_n. At the low frequencies, the values are scattered and generally large for the quadratic fit. The value of γ_n gradually increases as the frequency increases, but it is still negative. Above 120 cm^{-1}, γ_n becomes positive and almost constant about +1. At high-frequency tail states, the values are scattered again but much less than at low ones. The general trend of the Grüneisen parameters of a-Ge is similar to what have been determined for a-Si [9] but the spreading of the parameters in a-Ge is much less than that of a-Si.

The large dispersion of γ_n at the low- and high-frequency ranges in a-Si is explained in terms of over- and under-coordinated atoms [9]. However, the model used here is perfectly coordinated and thus the scattering at the tail states in a-Ge cannot be due to the coordination defects and it is probably related to the strained topology and/or the finite size of the system.

3.4. Thermal expansion

The negative Grüneisen parameters imply a negative thermal expansion $\alpha(T)$ of a-Ge. The computed parameters can be used to estimate the temperature dependence of $\alpha(T)$. The thermal expansion can be calculated using the following equation:

$$\alpha(T) = \frac{1}{3BV}\sum_a C_a\gamma_a,$$

where $C_a = k_B(\hbar\omega_a/k_BT)^2 n_a(n_a+1)$ is the specific heat of a harmonic oscillator, k_B is the Boltzman constant, B is the isothermal bulk modulus, V is the volume, and $n_a(\omega)$ is the average phonon population as given by the Bose–Einstein distribution
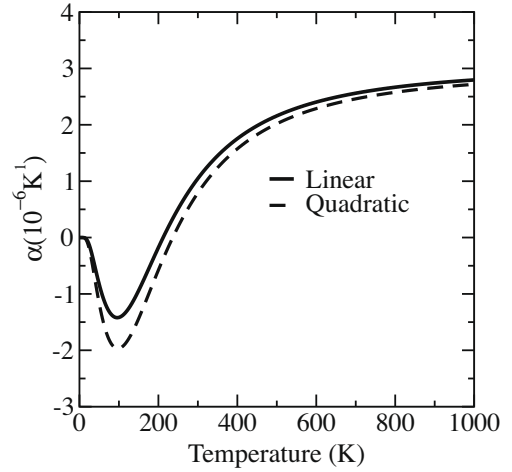

Fig. 3. Calculated thermal expansion.

$n_a(\omega) = [\exp(\hbar\omega/k_BT) - 1]^{-1}$. The calculated thermal expansion of a-Ge is illustrated in Fig. 3. Accordingly, the model shows a dramatic negative expansion below 200 K. The magnitude of expansion calculated from the quadratic fit is more than that of the linear fit because of the large negative value of Grüneisen parameters.

3.5. Phase quotient

In a crystal, vibrations can be explained with acoustic and optic phonons. In acoustic modes, neighboring atoms move in phase while in optic modes the motion is out of phase. In amorphous materials, the atomic vibrations cannot be characterized with a definite wave vector, and a division of atomic vibration into acoustic and optic phonons is not possible in general [10]. However, some characteristics can be calculated for vibrational modes in amorphous materials. One of the useful quantities is the phase quotient. The phase relationship between vibrations of neighboring atoms can be explained with the phase quotient $PQ(\omega_n)$ [41]:

$$PQ(\omega_n) = \frac{\sum_m \mathbf{u}_n^i \cdot \mathbf{u}_n^j}{\sum_m \left|\mathbf{u}_n^i \cdot \mathbf{u}_n^j\right|},$$

where atoms i and j constitute the mth bond, $\mathbf{u}_n^i$ is the displacement of atom i from its equilibrium position when it vibrates in mode n and the summation is over all nearest-neighbor bonds in the cluster. In terms of values of the phase quotient, it is possible to talk about acoustic-like and optic-like modes in amorphous materials. In acoustic-like modes, the motion of atom i and j is roughly in phase and the $PQ(\omega_n)$ is close to +1 and in optic-like phonons, the relative motion of atoms is roughly antiparallel for each pair and the $PQ(\omega_n)$ is around −1. The calculated $PQ(\omega_n)$ is illustrated in Fig. 4. At zero-pressure, the vibrations with $\omega < 120$ cm^{-1} are close to unity, indicating an acoustic-like nature of these eigenmodes. On the other hand, the high frequency spectral tail states are mainly negative and are regarded as optic-like vibrations. An abrupt change around 120 cm^{-1} in the $PQ(\omega_n)$ indicates that the different character of vibrations is separated by the band gap. The $PQ(\omega_n)$ tends to decrease in the low-frequency range with the application of pressure. This means that the mode mixing of the low-frequency vibrations occurs in response to pressure. At the transition, the abrupt change near 120 cm^{-1} disappears, and the $PQ(\omega_n)$ is found to be ⩽0.5, indicating a more optic-like character of the eigenmodes. The results reveal that pressure has a strong effect on the acoustic-like nature of the vibrations and even changes their character while having almost no effect on the optic-like vibrations. The gen-
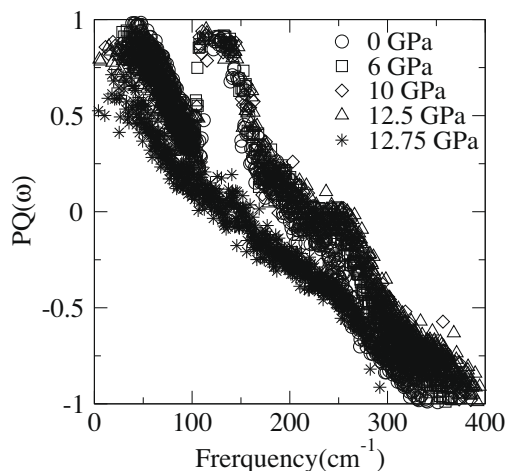
Fig. 4. The phase quotient. The PQ is close to +1 for acoustic-like modes and it is around −1 for optic-like modes.

eral features of the $PQ(\omega_n)$ of a-Ge and its behavior under pressure are very similar to those of a-Si [5,11].

3.6. Stretching character

Another useful quantity, introduced in Ref. [11], the stretching character $S(\omega_n)$ can be given by

$$S(\omega_n) = \frac{\sum_m |(\mathbf{u}_n^i - \mathbf{u}_n^j) \cdot \mathbf{r}^m|}{\sum_m |\mathbf{u}_n^i - \mathbf{u}_n^j|},$$

where $\mathbf{r}^m$ is a unit vector in the direction of the mth bond. When $S(\omega_n)$ is close to unity mode n is predominantly of bond stretching character while values close to zero imply bond bending modes.

The pressure dependence of $S(\omega_n)$ is given in Fig. 5. At zero-pressure, the modes less than 120 cm^{-1} have a bond bending character while those above 120 cm^{-1} have a bond stretching character. We find almost no change in the nature of the low- and high-frequency vibrations, but do find the mixing of modes near the band gap. As the system undergoes the phase transition, all modes become a more bond stretching character, similar to the behavior of a-Si [5].
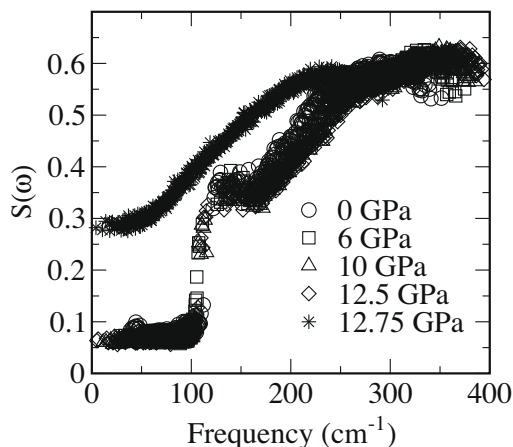

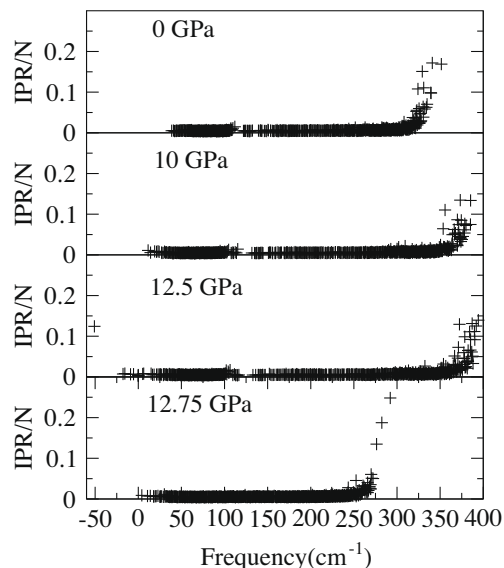**Fig. 5.** The stretching character of the vibrational modes.

Fig. 6. The inverse participation ratio of the a-Ge model under pressure.

3.7. Localized states and response to pressure

Structural disorder causes localized modes. The usual measure of the degree of localization of vibrational modes is the inverse participation ratio (IPR),

$$\text{IPR}^{-1}(\omega_n) = N \frac{\sum_{j=1}^N (\mathbf{u}_n^j \cdot \mathbf{u}_n^j)^2}{\left[\sum_{j=1}^N (\mathbf{u}_n^j \cdot \mathbf{u}_n^j)\right]^2},$$

where N is the number of atoms in the supercell and $\mathbf{u}_n^j$ is the displacement of atom j from its equilibrium position. The IPR will have a value of ~ 1 for an extended mode where all atoms contribute equally and a value of $1/N$ for a mode defined by only one atom. In Fig. 6, we show the IPR of a-Ge under pressure. The larger the IPR for a state, the more spatially localized it is. At zero-pressure, the highest frequency modes are localized and characterized by large values of the inverse participation ratio. The localized states are mostly associated with a large deviation of bond angles from the ideal tetrahedral angle and the long bond lengths that are longer than the average. The application of pressure shortens these bonds and hence reduces the number of localized states. The localized states preserved under the pressure are due to the angular distortions. Pressure-induced delocalization has been observed in various systems in a-Si [5], a-GeSe$_2$ [6] and SiO$_2$ [7].

4. Discussion

We have found that the acoustic-like eigenmodes of a-Ge soften under pressure, resulting negative Grüneisen parameters. On the other hand, the optic-like frequencies shift to higher frequencies, which is in good agreement with the recent Raman investigations [22,45]. The optic-like modes have positive Grüneisen parameters. Regrettably, we are not able compare some of our results with experiments because there is no information reported in the literature about the response of the low-frequency modes of a-Ge to pressure and Grüneisen parameters of a-Ge. However, the behavior of the optic-like and acoustic-like frequencies of a-Ge as a function of pressure is similar to what has been observed in crystalline Ge [46–48]. Furthermore, the TA(X) and TO(Γ) modes of crystalline Ge have negative (−1.53) [47] and positive (1.14) [48] Grüneisen parameters, respectively.

We also observe a negative thermal expansion below 200 K but again are not able to compare this result with experiment because we are not aware of any experimental studies on the thermal expansion of pure *a*-Ge. However, earlier studies on crystalline Ge [49,50] reveal that it shows the negative thermal expansion and hence such a tendency is also expected in amorphous Ge.

We should note here that the studies have revealed that the magnitude of the expansion strongly depends on sample preparation technique, i.e., structure of disordered systems. The thermal expansion of hydrogenated amorphous Ge is about three times larger than crystalline Ge between 300 and 420 K [51]. Furthermore, Fabian and Allen [9] have shown that the $\alpha(T)$ of *a*-Si varies with the size of the models in addition to their topologies. Therefore, the dramatic thermal expansion of *a*-Ge observed in the present study might be associated with the topology of the initial structure and the size of the simulation cell. Additionally, the use of linear and quadratic fittings to calculate Grüneisen parameters might results in some errors in our calculations, which also lead to some errors to predict the magnitude of the thermal expansion.

5. Conclusions

The vibrational properties of *a*-Ge under pressure have been studied using *ab initio* constant-pressure relaxation simulations. The calculations reveal the pressure-induced phonons softening at the low-frequency range with a decrease in their acoustic-like nature. On the other hand the high-frequency vibrations gradually shift to higher energies. The acoustic-like phonons have negative Grüneisen parameters while the optic-like ones have positive parameters. A negative thermal expansion is observed below 200 K. We also find the pressure-induced delocalization of the high-frequency tail states. As the system undergoes a phase transition into a metallic high-density amorphous phase the bond bending and acoustic nature of phonons are lost.

Acknowledgements

References

[1] S. Lannin, L.J. Pilione, S.T. Kshirsagar, R. Messier, R.C. Ross, Phys. Rev. B 26 (1982) 3505.
[2] N. Maley, J.S. Lannin, Phys. Rev. B 36 (1987) 1146.
[3] N. Maley, D. Beeman, J.S. Lannin, Phys. Rev. B 38 (1988) 10611.
[4] D. Beeman, R. Tsu, M.F. Torpe, Phys. Rev. B 32 (1985) 874.
[5] M. Durandurdu, D.A. Drabold, Phys. Rev. B 66 (2002) 155205.
[6] M. Durandurdu, D.A. Drabold, Phys. Rev. B 65 (2002) 104208.
[7] W. Jin, R.K. Kalia, P. Vashishta, J.P. Rino, Phys. Rev. Lett. 71 (1993) 3146.
[8] F. Finkemeier, W. von Niessen, Phys. Rev. B 58 (1998) 4473.
[9] J. Fabian, P.B. Allen, Phys. Rev. Lett. 79 (1997) 1885.
[10] S.N. Taraskin, S.R. Elliot, Phys. Rev. B 56 (1997) 8605.
[11] M. Marinov, N. Zotov, Phys. Rev. B 55 (1997) 2938.
[12] R. Alben, D. Weaire, J.E. Smith, M.H. Brodsky, Phys. Rev. B 11 (1975) 2271.
[13] G. Fanchini, A. Tagliaferro, G. Messina, S. Santangelo, A. Paoletti, A. Tucciarone, J. Appl. Phys. 91 (2002) 1155.
[14] D. Beeman, R. Alben, Adv. Phys. 26 (1977) 339.
[15] P.H. Poole, T. Grande, F. Sciortino, H.E. Stanley, C.A. Angle, Comput. Mater. Sci. 4 (1995) 373.
[16] O. Mishima, L.D. Calvert, W. Whalley, Nature (London) 314 (1985) 76.
[17] M. Durandurdu, D.A. Drabold, Phys. Rev. B 64 (2001) 014101.
[18] P.F. McMillan, M. Wilson, D. Daisenberger, D. Machon, Nat. Mater. 4 (2005) 680.
[19] S.D. Daisenberger, M. Wilson, P.F. McMillan, P.F. McMillan, R. Quesada Cabrera, M.C. Wilding, D. Machon, Phys. Rev. B 75 (2007) 224118.
[20] P.F. McMillan, J. Matter. Chem. 14 (2004) 1506.
[21] M. Durandurdu, D. Drabold, Phys. Rev. B 66 (2002) 041201.
[22] A. Di Cicco, A. Congeduti, F. Coppari, J.C. Chervin, F. Baudelet, A. Polian, Phys. Rev. B 78 (2008) 033309.
[23] E. Principi, A. Di Cicco, F. Decremps, A. Polian, S. De Panfilis, A. Filipponi, Phys. Rev. B 69 (2004) 201201.
[24] J. Koga, K. Nishio, T. Yamaguchi, F. Yonezawa, J. Phys. Soc. Jpn. 73 (2004) 388.
[25] C. Meade, R.J. Hemley, H.K. Mao, Phys. Rev. Lett. 69 (1992) 1387.
[26] L. Huang, J. Kieffer, Phys. Rev. B 69 (2004) 224203.
[27] K. Tanaka, J. Non-Cryst. Solids 90 (1987) 370.
[28] Q. Mei, C.J. Benmore, R.T. Hart, E. Bychkov, P.S. Salmon, C.D. Martin, F.M. Michel, S.M. Antao, P.J. Chupas, P.L. Lee, S.D. Shastri, J.B. Parise, K. Leinenweber, S. Amin, J.L. Yarger, Phys. Rev. B 74 (2006) 014203.
[29] S.M. Antao, C.J. Benmore, B. Li, L. Wang, E. Bychkov, J.B. Parise, Phys. Rev. Lett. 100 (2008) 115501.
[30] K. Miyauchi, J. Qiu, M. Shojiya, Y. Kawamoto, N. Kitamura, J. Non-Cryst. Solids 186 (2001) 279.
[31] S.K. Lee, P.J. Eng, Ho-Kwang Mao, Y. Meng, M. Newville, M.Y. Hu, Jinfu Shu, Nat. Mater. 4 (2005) 851.
[32] V.V. Brazhkin, Y. Katayama, K. Trachenko, O.B. Tsiok, A.G. Lyapin, E. Artacho, M. Dove, G. Ferlat, Y. Inamura, H. Saitoh, Phys. Rev. Lett. 101 (2008) 035702.
[33] S. Sen, S. Gaudio, B.G. Aitken, C.E. Lesher, Phys. Rev. Lett. 97 (2006) 025504.
[34] O.B. Tsiok, V.V. Brazhkin, A.G. Lyapin, L.G. Khvostantsev, Phys. Rev. Lett. 80 (1998) 999.
[35] V.V. Brazhkin, A.G. Lyapin, J. Phys.: Condens. Matter 15 (2003) 6059.
[36] M. Durandurdu, Phys. Rev. B 79 (2009) 205202.
[37] M. Durandurdu, Phys. Rev. B 73 (2006) 035209.
[38] G.T. Barkema, N. Mousseau, Phys. Rev. B 62 (2000) 4985.
[39] O.F. Sankey, D.J. Niklewski, Phys. Rev. B 40 (1989) 3979.
[40] H.S. Chen, D. Turnbull, J. Appl. Phys. 40 (1969) 4214.
[41] P. Germain, K. Zellama, S. Squelard, J.C. Bourgoin, A. Gheorghiu, J. Appl. Phys. 50 (1979) 6986.
[42] M. Durandurdu, Phys. Rev. B 71 (2005) 054112.
[43] M. Parrinello, A. Rahman, Phys. Rev. Lett. 45 (1980) 1196.
[44] D.J. Lacks, Phys. Rev. Lett. 80 (1998) 5385.
[45] F. Coppari, J.C. Chervin, A. Congeduti, M. Lazzeri, A. Polian, E. Principi, A. Di Cicco, Phys. Rev. B 80 (2000) 115213.
[46] B.R. Wu, Chin. J. Phys. 44 (2006) 454.
[47] D. Olega, M. Cardona, Phys. Rev. B 25 (1982) 1151.
[48] S. Klotz, J.M. Besson, M. Braden, K. Karch, P. Pavone, D. Strauch, W.G. Marshall, Phys. Rev. Lett. 79 (1997) 1313.
[49] P. Fornasini, S.I. Ahmed, A. Sanson, M. Vaccari, Phys. Stat. Sol. 245 (2008) 2497.
[50] T. Soma, J. Phys. Soc. Jpn. 42 (1977) 1491.
[51] P.D. Persans, A.F. Ruppert, J. Appl. Phys. 1 (1986) 271.